Molecular Cell
Article

The Structure of the C-Terminal Domain of the Protein Kinase *At*SOS2 Bound to the Calcium Sensor *At*SOS3

María José Sánchez-Barrena,[1] Hiroaki Fujii,[2,3] Ivan Angulo,[1] Martín Martínez-Ripoll,[1] Jian-Kang Zhu,[2,3] and Armando Albert[1,*]
[1] Grupo de Cristalografía Macromolecular y Biología Estructural, Instituto de Química Física "Rocasolano," Consejo Superior de Investigaciones Científicas, Serrano 119, Madrid E-28006, Spain
[2] Department of Botany and Plant Sciences
[3] The Institute for Integrative Genome Biology
2150 Batchelor Hall, University of California, Riverside, Riverside, CA 92521, USA
*Correspondence: xalbert@iqfr.csic.es
DOI 10.1016/j.molcel.2007.04.013

SUMMARY

The plant SOS2 family of protein kinases and their interacting activators, the SOS3 family of calcium-binding proteins, function together in decoding calcium signals elicited by different environmental stimuli. SOS2 is activated by Ca-SOS3 and subsequently phosphorylates the ion transporter SOS1 to bring about cellular ion homeostasis under salt stress. In addition to possessing the kinase activity, members of the SOS2 family of protein kinases can bind to protein phosphatase 2Cs. The crystal structure of the binary complex of Ca-SOS3 with the C-terminal regulatory moiety of SOS2 resolves central questions regarding the dual function of SOS2 as a kinase and a phosphatase-binding protein. A comparison with the structure of unbound SOS3 reveals the basis of the molecular function of this family of kinases and their interacting calcium sensors. Furthermore, our study suggests that the structure of the phosphatase-interaction domain of SOS2 defines a scaffold module conserved from yeast to human.

INTRODUCTION

The coordinated action of protein kinases and phosphatases produces transient phosphorilation, a regulatory mechanism by which living organisms control cellular processes in response to developmental, hormonal, and environmental cues. Given the importance of such processes, the activity of these proteins must be under tight regulation to ensure the integration of diverse biological stimuli and the generation of appropriate cellular responses. Protein-protein interactions are fundamental to understand this regulation and signal transfer mechanisms of signal transduction. Protein kinases have evolved to display discrete scaffold domains or even short sequence motives to interact with their binding partners and regulate their function.

SOS2 is a serine/threonine protein kinase that is required for plant salt tolerance (Halfter et al., 2000; Liu et al., 2000; Zhu, 2000, 2003; Guo et al., 2001; Guo et al., 2004). SOS2 physically interacts with the calcium sensor SOS3 (Liu and Zhu, 1998) and is activated by it (Halfter et al., 2000). The binding of SOS2 to SOS3 is mediated by the 21 amino acid FISL motif in SOS2, which is autoinhibitory to the kinase activity (Guo et al., 2001). SOS2 displays its activity at the plasma membrane where the SOS2-SOS3 kinase complex is required for the phosphorylation and activation of the Na^+/H^+ antiporter SOS1 (Qiu et al., 2002; Quintero et al., 2002). The myristoylation of SOS3 at its N terminus is important for recruiting SOS2 to the lipid bilayer (Ishitani et al., 2000; Quintero et al., 2002). In addition, it is known that SOS2 can interact with the PP2C-type protein phosphatase ABI2 through a 33 amino acid sequence designated as the PPI-binding motif (Ohta et al., 2003). The FISL and PPI motifs are located in the C-terminal regulatory region of the SOS2 kinase.

SOS2 and SOS3 are the founding members of a unique protein family in *Arabidopsis* of 25 kinases that contain FISL (also known as NAF) and PPI motifs, the PKS or CIPKs (thereafter CIPKs) (Guo et al., 2001), and of a family of ten EF-hand-type calcium-binding proteins, the SCaBPs (Guo et al., 2001) or CBLs (thereafter CBLs) (Luan et al., 2002), respectively. These proteins are proposed to decode specific calcium signals triggered by a number of extracellular stimuli such as salinity, drought, cold, gravity, light, anoxia, and mechanical perturbation (Harmon et al., 2000; Scrase-Field and Knight, 2003).

The mechanisms conferring signaling specificity to this network of proteins appear to rely on the differential calcium-binding affinities of the CBLs, the differential expression pattern and subcellular localization of both the CIPKs and CBLs, and the interaction specificity in CBL-CIPK combinations. Although these issues have been investigated (Gong et al., 2004; Batistic and Kudla, 2004) and the crystal structures of SOS3 (Sanchez-Barrena et al., 2005) and CBL2 (Nagae et al., 2003) in the presence of

calcium have been determined, the molecular mechanism underlying CBL-mediated activation of the CIPKs and the selectivity of each CBL-CIPK interacting partner remains obscure.

Recently, it has been reported that CIPK23, interacting with the calcium-binding proteins CBL1 and CBL9, regulates the *Arabidopsis* ion transporter AKT1 (Xu et al., 2006; Li et al., 2006). Available data suggest a general mechanism in which CBL-CIPK complexes may be regulating the phosphorylation state of various ion transporters. Moreover, the ability of SOS2 to interact with the protein phosphatase ABI2 suggests that SOS2-ABI2 and/or other CIPK-PP2C complexes could act as molecular on-off switches controlling the phosphorylation state of plant ion transporters. However, little is known currently about the regulation of the opposite activities of the kinase and phosphatase that should be under tight regulation so that they do not occur simultaneously.

To understand the molecular architecture of the CIPK-CBL interaction, we have determined the X-ray crystallographic structure of the complex between the C-terminal regulatory moiety of the kinase SOS2 and the calcium-binding protein SOS3. The structure provides a molecular basis of CBLs-mediated activation of CIPKs and insights into the molecular mechanism conferring specificity to the interaction. The structure also suggests a mechanism for the control of the phosphatase-binding and kinase activities of CIPKs and, consequently, for the regulation of various plant ion transporters.

RESULTS AND DISCUSSION

Overall Structure of the Complex

The crystal structure of the complex between the calcium-binding protein SOS3 and the C-terminal regulatory moiety of SOS2 (C-SOS2, residues 306–430) was determined at 2.0 Å resolution (see Table 1 and the Experimental Procedures section for further details). The crystallographic analysis revealed a single copy of a SOS3:C-SOS2 heterodimer in the asymmetric unit. The complex comprises two distinct structural domains connected by a short polypeptide (Figure 1). SOS3 and the FISL/NAF motif from SOS2 (residues 311–321) form a single domain. In this domain, SOS3 defines a long binding cleft where the FISL/NAF motif is placed and displays an extended conformation. The other structural domain is formed by the SOS2 residues from 339 to 430. They are folded to form a five-stranded antiparallel β sheet and two α helices. We designate this domain the protein phosphatase interaction (PPI) domain since it includes the SOS2 PPI motif that interacts with the PP2C-type protein phosphatase ABI2.

The PPI domain packs against the SOS3-FISL/NAF domain and lies in the opposite side of the SOS3 calcium-binding sites. It makes contacts with the accessible residues of the N-terminal moiety of the FISL/NAF motif and the surrounding residues of SOS3. The overall architecture of the complex resembles that of the calcineurin/cyclophilin and calcineurin/FKBP12 complexes (Jin and Harrison, 2002; Kissinger et al., 1995) (see Figure S1 in the Supplemental Data available with this article online). The complex is largely stabilized by hydrophobic intermolecular interactions between both polypeptide chains since more than 75% of the buried surface area is formed by nonpolar atoms (2650 Å^2 of 3487 Å^2). Both the interactions between SOS3 and FISL/NAF motif and between SOS3 and PPI domain contribute to the formation of the complex (66% and 34% of the total buried surface area, respectively) (Wallace et al., 1995).

Table 1. Data Collection and Refinement Statistics

Data Collection	
Space group	$P2_12_12_1$
Cell dimensions	
a, b, c (Å)	44.14, 57.39, 141.90
α, β, γ (°)	90.0, 90.0, 90.0
Resolution (Å)	70.9–2.00 (2.05–2.00)
R_{sym}	0.06 (0.35)
I/σ(I)	9.7 (2.6)
Completeness (%)	99.3 (92.7)
Redundancy	4.4 (3.5)
Refinement	
Resolution (Å)	70.0–2.00 (2.05–2.00)
Number of reflections	23,719
R_{work}/R_{free}	21.5/25.9 (28.6/32.6)
Number of atoms	
Protein	2722
Calcium ion	2
Water molecules	211
Average B factors	33.67
Rmsd	
Bond lengths (Å)	0.013
Bond angles (°)	1.388
B factors	1.523
Ramachandran plot statistics	90.8% in the core
	9.2% in the allowed

Highest-resolution shell is shown in parentheses.
$R_{sym} = \Sigma_{hkl}|I_{hkl} - \langle I_{hkl}\rangle|/\Sigma_{hkl}I_{hkl}$.

The SOS3-FISL/NAF Domain

The overall structure of the SOS3 portion of the complex is formed by two pairs of EF hand motifs. This structure appears to be the same as that described previously for the unbound form of SOS3 (Sanchez-Barrena et al., 2005) and the homologous CBL2 (Nagae et al., 2003). However, a comparison of these structures shows that large differences arise form the relative position of the helices F4 and E4, connecting EF hands 3 and 4, and the loop

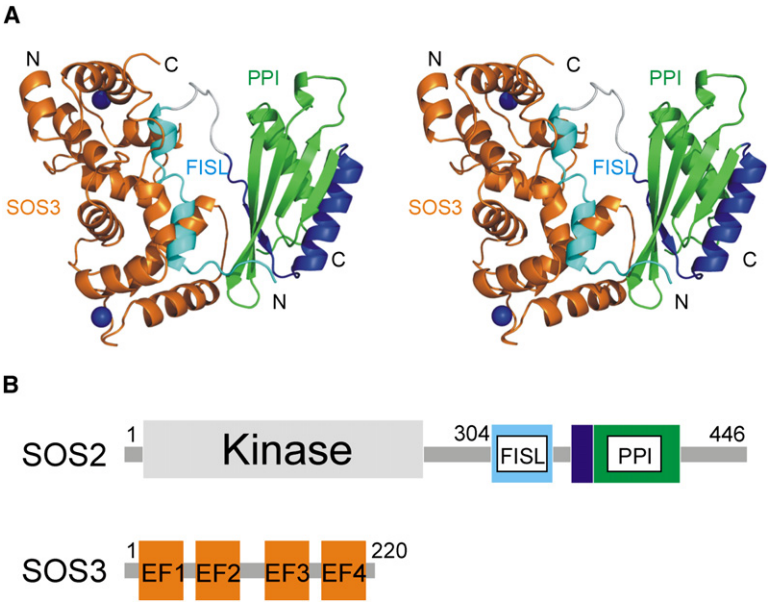

Figure 1. The Crystal Structure of SOS3 and the C-Terminal Regulatory Domain of SOS2

(A) Stereoview of the ribbon representation of the structure. SOS3 is displayed in orange, the FISL/NAF motif is displayed in cyan, the PPI motif is displayed in blue, and the rest of the PPI domain of SOS2 is displayed in green. Calcium atoms are displayed as blue spheres. (B) Domain structure of SOS2 and SOS3. The domains have been colored as in (A).

between helices F1 and E1, connecting EF hands 1 and 2 (Figure 2A and Movie S1). These rearrangements yield to a SOS3 molecule displaying an open conformation that is able to bind the FISL/NAF motif.

The FISL/NAF motif fits remarkably well in the binding cleft formed by SOS3. The stability of the complex is maintained by means of hydrophobic interactions, involving 12 hydrophobic side chains for SOS3 and seven for the FISL/NAF motif. In addition, five hydrogen bonds strengthen the interaction (see Figure 3 and Figure S2). This architecture provides the structural basis for the SOS2 kinase regulation. Biochemical data showed that SOS2 protein kinase domain binds to the FISL/NAF motif and that this interaction is responsible for the inhibition of its kinase activity (Guo et al., 2001). The structure shows that the FISL/NAF motif would not be accessible to the kinase domain if it is bound to SOS3, leaving the kinase active.

The recognition mode of SOS3 and the FISL/NAF motif resembles that observed for the regulatory and catalytic subunits of calcineurin (CnB and CnA) (Kissinger et al., 1995) and that observed for the human calcineurin B homologous protein (CHP2) and the plasma membrane Na/H exchanger (NHE) (Ben-Ammar et al., 2006). In these structures, the CnA- and NHE-binding segments expand a single α-helical motif onto the CnB and CHP2 subunits, respectively. In comparison, the FISL/NAF motif consists of two small α-helical segments, each one bound to an EF hand pair (helices αFIS1 and αFIS2) and flanked by short peptides (Figure 2B).

The SOS3-FISL/NAF structure together with a sequence analysis of the CIPK family reveals that the conserved residues among the proteins of the family are responsible for the overall shape of the FISL/NAF motif (Figure S3). In particular, Asn311, Ala312, Phe313, Ile316, Ser319, and Leu322 from the SOS2 FISL/NAF motif are highly conserved among the CIPK family (hence the name FISL/NAF motif). Interestingly, Asn311, Ala312, and Phe313 are involved in the formation of the loop connecting the N terminus of the FISL/NAF motif and the αFIS1 and Ile316, Ser119, and Leu322 and stabilize the central loop of the FISL/NAF motif (Figure S3). All these residues are buried in the C-SOS2:SOS3 interaction (Figure 3B). These data suggest that the particular folding of the SOS2 FISL/NAF domain is shared with other members of the CIPK family. This may explain the selectivity of CBL toward the CIPK family but not other protein families.

The specificity of the interaction between the CIPKs and CBLs has been extensively investigated both in vivo and in vitro. These studies revealed that some CBLs can interact with multiple CIPKs but that some others can only interact with a particular CIPK (Guo et al., 2001; Gong et al., 2004; Batistic and Kudla, 2004). The sequence variation within the FISL/NAF motifs and/or in the neighboring residues of the target kinases probably determines the specificity between CIPKs-CBLs pairs. However, this would not fully explain the specificity of the interaction, as the most variable residues among the FISL/NAF motifs are solvent accessible residues that do not interact with SOS3 (Figure 3B). These residues, such as Gln320 and Asn323 (Figure S3), are placed in the loop connecting the α-helical segments of the FISL/NAF motif, and they are stabilizing the relative position of the α-helical segment bound to the N-terminal EF hand pair domain with respect to the C-terminal one. Since the analysis of the structures of the unbound forms of SOS3 and CBL2 shows that the differences can be described as a hinge motion between the N-terminal and C-terminal EF hand pairs (Sanchez-Barrena et al., 2005), this suggests that the particular conformation of each FILS/NAF motif and the relative position of the EF hand pairs of each CBL should provide the

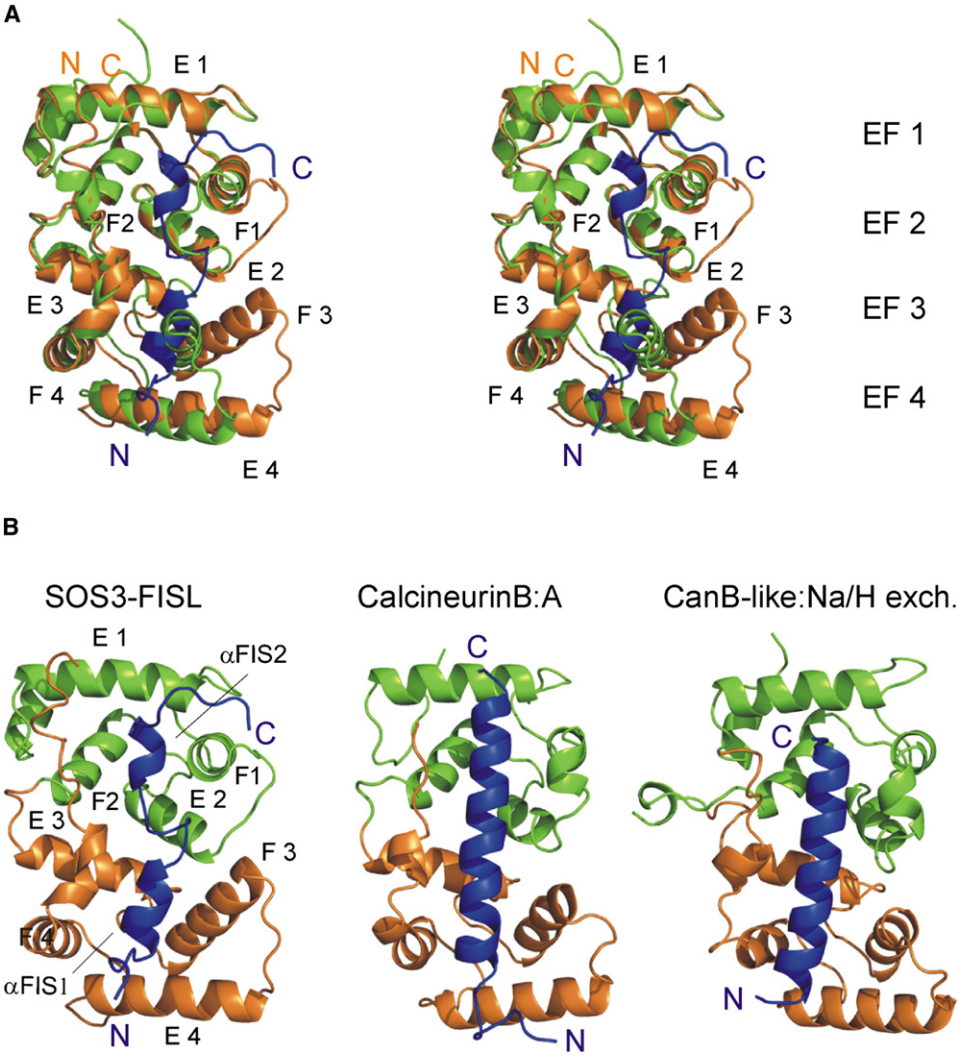

Figure 2. Structural Comparison of SOS3 and Related Structures

(A) Stereoview of the superimposition of the ribbon diagrams corresponding to the structures of the SOS3-FISL/NAF domain (orange/blue) and the unbound form of SOS3 (green) (PDB code 1V1G).

(B) Structure of the SOS3-FISL/FISL domain (left) and the structurally related complexes is shown: the regulatory and catalytic subunits of calcineurin (center, PDB code 1TCO) and the cacineurin B homologous protein and the plasma membrane Na/H exchanger (right, PDB code 2BEC).

structural basis for the specificity of the CBLs-CIPKs interaction.

The high-resolution electron density map allowed the positioning of two calcium atoms at sites EF1 and EF4 and to model unambiguously the structure of the four calcium-binding sites. In contrast, the structure of the unbound form of SOS3 shows that the four EF hands are fully occupied with calcium. Consequently, it is difficult to see how calcium promotes the binding of SOS3 to SOS2 and how it stimulates the kinase activity from the comparison of both structures. To address this question, sedimentation equilibrium experiments were performed to investigate the effect of calcium in the association state of C-SOS2:SOS3 in solution (see the Experimental Procedures for details). Our data show that calcium stabilizes a heterodimeric C-SOS2:SOS3 complex in solution. On the other hand, the sample precipitates, becomes polydisperse, and/or forms high molecular weight aggregates when the same analysis is carried out in the presence of a chelating agent such as EDTA. The structure of the complex shows that the EF4 binding site should be the closest to the kinase domain, suggesting that the calcium binding to this site may be responsible of the activation of the kinase. Indeed, solution studies demonstrate that this site is able to interchange calcium with the media (Sanchez-Barrena et al., 2005). A local change in the structure motivated by calcium binding could be responsible for global changes in the structure, as has been reported for other EF hand proteins (Lewit-Bentley and Rety, 2000; Otterbein et al., 2002).

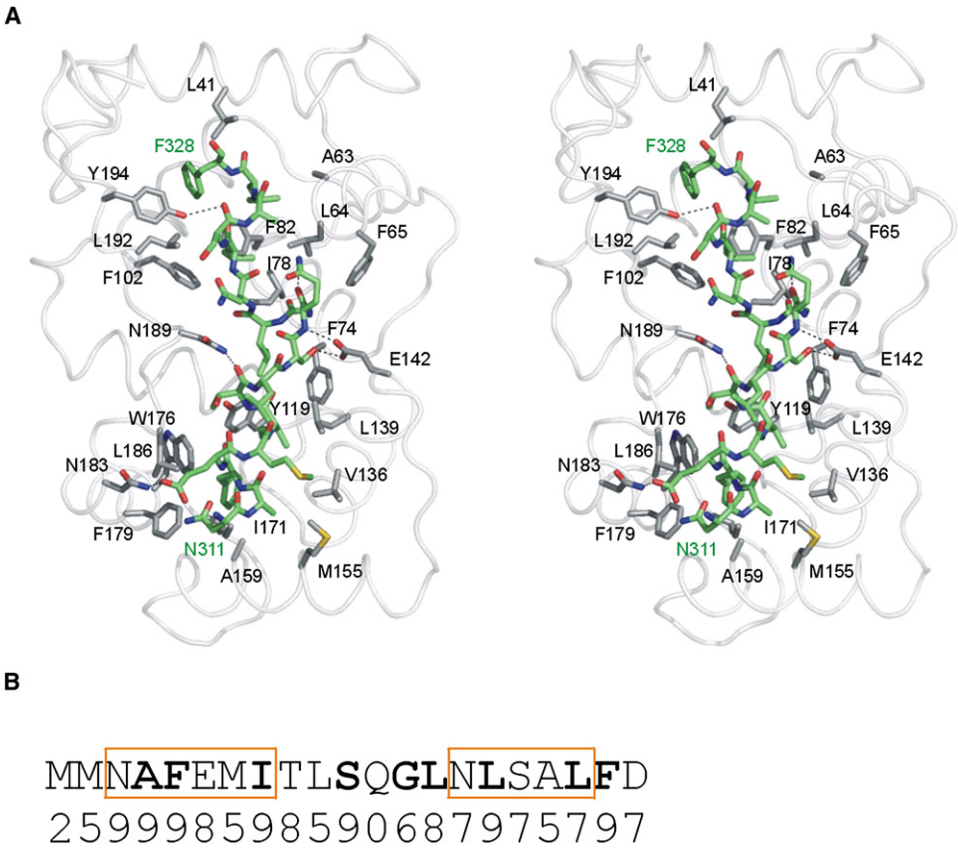

Figure 3. Interactions between the SOS2 FISL/NAF Motif and SOS3

(A) Stereodiagram showing the interactions between SOS2 FISL/NAF motif (green carbon atoms) and SOS3 (white carbon atoms). The SOS3 labeled residues are within a 3.8 Å sphere around SOS2 FISL/NAF motif. The straight dashed lines stand for the hydrogen bonds.

(B) FISL/NAF motif amino acid sequence. Residues depicted in bold are totally buried in the interaction with SOS3. The boundaries of the α helices forming the motif are also indicated as orange rectangles. The residue conservation degree among the members of the CIPK family is indicated as a numerical value: 9, conserved residue; 0, highly variable residue (Landau et al., 2005).

The Structure of the PPI Domain

The PPI domain folds as an α/β domain in which two α helices pack against a five-stranded antiparallel β-sheet with a β1-β5-β4-β3-β2 strand order. The first α helix (α1) connects β1 and β2, and the second (α2) is placed between β5 and the C-terminal end. The length of the β strands varies along the β sheet, with β5 and β4 double the size of β1, β3, and β2. The C terminus of the strand β1 aligns with the N terminus of the β5, whereas the β3 and β2 align with the N terminus of the β4. The protein phosphatase-binding sequence spans along the strand β1 and the first α helix of the domain (Figure 4A).

In the PPI motif of SOS2, the residues in the vicinity of the loop connecting β1 and α1 are highly conserved (Landau et al., 2005) among the protein of the CIPK family, suggesting that they are structurally and functionally important regions for phosphatase binding (Figure 4B). Indeed, targeted mutations of the conserved Arg340 and Phe341 abolished phosphatase binding (Ohta et al., 2003). On the other hand, the most variable residues are located in the tip of the loop. This suggests that the variations in the loop may confer the specificity of a particular kinase for a particular phosphatase.

The PPI domain structure shows a striking similarity with that of the kinase associated domain 1 (KA1) of mouse map/microtubule affinity-regulating kinase 3 (MARK3) (Tochio et al. [2006], part of the Japanese Structural Genomic Project, PDB code 1UL7), although the sequence identity between them is very low (less than 14%). The Cα backbone of the PPI domain structure closely superimposes on the corresponding one of KA1, with a root-mean-square deviation of 1.54 Å for a total of 74 structurally equivalent Cα atoms (Figure 4C) (CCP4, 1994). MARK3 protein kinase belongs to the KIN2/PAR-1/MARK subfamily of protein kinases, which are conserved from yeast to human. As it is observed for the PPI domain of CIPKs, the members of the family display the KA1 domain in the C-terminal end of the protein. Members of this kinase subfamily are involved in various biological processes such as cell polarity regulation, cell cycle control, intracellular signaling, microtubule stability, and protein stability (Tassan and Le Goff, 2004). Although the function of the KA1 domain is not yet

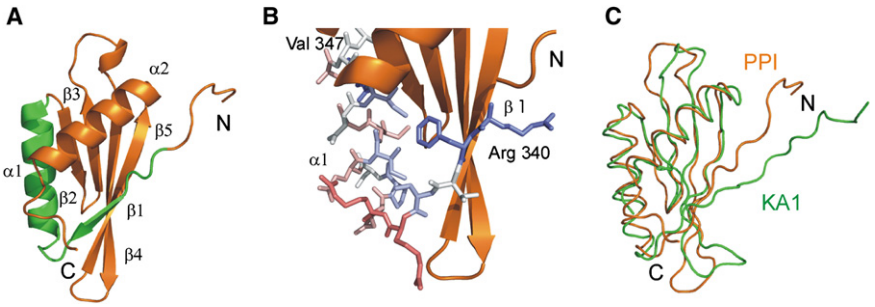

Figure 4. The Structure of the PPI Domain and Related Structures

(A) A ribbon representation of the PPI domain structure. The PPI module is depicted in green.

(B) A section of the structure. The residues belonging to the PPI module are represented in a stick mode. These residues are colored according to their conservation degree among the members of the CIPK family. Blue, conserved residue; red, variable residue (Landau et al., 2005).

(C) Superimposition of the diagrams corresponding to the structures of the PPI domain (orange) and the structurally related KA1 domain (green, PDB code 1UL7).

known, the structural similarity with PPI domain suggests a common function for both domains. In this sense, the structure of the SOS2 C-terminal domain would define a scaffold module involved in the interaction with protein phosphatases that is conserved from yeast to human.

Domain Organization of the Complex

The analysis of the domain architecture of the binary complex between the calcium-binding protein SOS3 and the C-terminal moiety of the kinase SOS2 resolves the important question about the regulation of the dual and opposite functions of the C-terminal moiety of SOS2: the control of the SOS2 kinase activity and the binding to ABI2 phosphatase. The major interactions between the SOS3-FISL/NAF and PPI domains involve residues form the loop connecting EF hands 3 and 4 in SOS3 and residues form the β sheet end formed by β1, β5, and β4 in the PPI domain (Figures 1 and 4A). In particular, Arg340 and Phe341, the residues that have been proven to be essential for ABI2 phosphatase binding, are buried in the interdomain interface (Figure 5). In fact, using two hybrid assays, Ohta et al. (2003) showed that mutations of these residues not only disrupt the interaction with the phosphatase ABI2 but also hinder the interaction with SOS3. In addition, the relative position of the SOS3-FISL/NAF domain and the PPI domain is restrained by both the linker connecting the FISL/NAF motif and the PPI domain and the interactions between the PPI domain and SOS3. This arrangement necessarily implies that a dissociation of the FISL/NAF motif from SOS3 should be coupled with the dissociation of PPI module from SOS3. All these data show that the binding of ABI2 and SOS3 to SOS2 is mutually exclusive. Indeed, this hypothesis was confirmed in a direct competition experiment. An in vitro MBP pull-down assay was performed using MBP-fused SOS2 (MBP-SOS2) (Figure 6). The preincubation of MBP-SOS2 with increasing amounts of His-tagged ABI2 (His-ABI2) yields to a reduction in the amount of GST-fused SOS3 (GST-SOS3) pulled down with MBP-SOS2. On the other hand, the preincubation with the control protein bovine serum albumin (BSA) did not reduce the amount of pulled down GST-SOS3. These observations support that the binding of SOS3 to SOS2 and the subsequent kinase activation are only possible when the SOS2 kinase is not interacting with ABI2.

In addition, the molecular architecture of the complex provides insights into the process by which the SOS2-SOS3 active complex is placed at the plasma membrane for the phosphorylation of the SOS1 ion transporter. The N-terminal myristoylation site of SOS3 and the N-terminal catalytic domain of SOS2 are placed in opposite sides of the complex. This configuration is compatible with the proposed role of SOS3 being the bridge between native SOS2 protein and the plasma membrane.

Implications and Conclusions

The signal transfer mechanisms of signal transduction are often mediated by scaffold modules and proteins that organize the signaling proteins into supramolecular complexes. These macromolecular arrangements ensure the

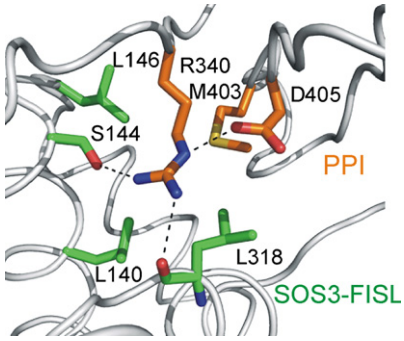

Figure 5. Relevant Interactions between the SOS3-FISL/NAF Domain and the PPI Domain

A section of the structure of the regulatory domain of SOS2 and SOS3 showing the residues interacting with Arg340. The labeled residues are within 3.8 Å sphere around Arg340. The straight dashed lines stand for the hydrogen bonds. Residues belonging to the SOS3-FISL/NAF domain are depicted in green. Residues belonging to the PPI domain are depicted in orange.

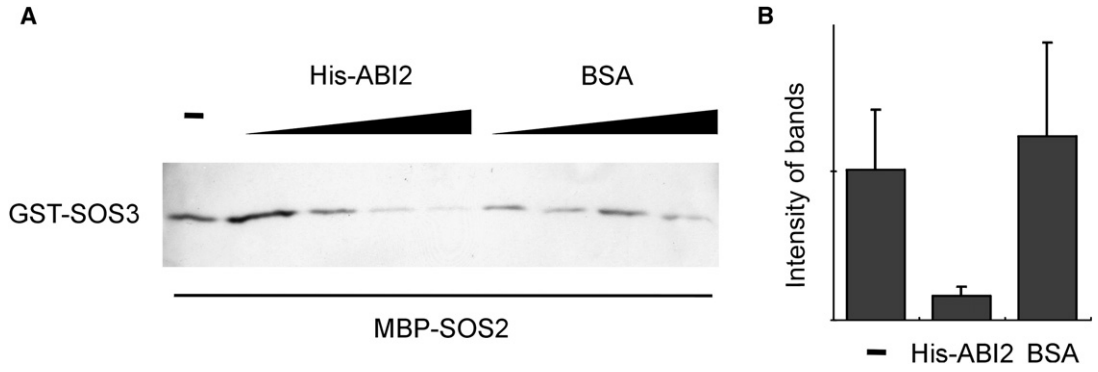

Figure 6. Competition between SOS3 and ABI2 for SOS2 Binding

(A) GST-SOS3 was pulled down with MBP-SOS2 that was preincubated with or without (–) different amounts of His-ABI2 or BSA. Triangles on the top symbolize the amount of His-ABI2 or BSA (0.2, 1.2, 6, and 30 μg). GST-SOS3 was detected by western blotting with anti-GST antibody.

(B) A bar diagram showing the quantitative analysis of the data presented in (A). The diagram shows the intensity of the bands without (–) or with 30 μg of His-ABI2 or BSA. The mean values are indicated (40, 6, and 49, respectively, in arbitrary units), and the standard deviations are represented as error bars. Calculations have been performed using four independent observations.

colocalization of the substrates and the products at particular cellular place, increase the specificity of the signal, and often are involved in the regulation of the activity of its components (Moscat et al., 2006). The CIPKs have evolved to display discrete modules that guarantee the fine decoding of specific calcium signals triggered by a number of extracellular stimuli.

The structure of the C-SOS2:SOS3 heterodimer provides the structural basis for the regulation of the SOS2 kinase activity and binding to the protein phosphatase 2C. Our data provide a molecular mechanism for the kinase activation in which the calcium sensor SOS3 opens a cavity and binds the SOS2 autoinhibitory FISL/NAF motif. The basis for this regulation should be conserved among the *Arabidopsis* protein network formed by the CBLs calcium sensors and CIPKs family of kinases. In addition, our work shows the molecular basis for the specificity of the CBL proteins for the CIPKs, and not for other protein kinases, and shed light on the mechanism that confers specificity to each CBL-CIPK pair.

On the other hand, the joined analysis of the structure and the biochemical data show that the binding of SOS2 to the phosphatase ABI2 would preclude the binding of SOS3 to SOS2 and subsequent kinase activation. The SOS2 PPI domain is blocked by SOS3, and this ensures that the opposite activities, kinase activity and phosphatase binding, cannot occur simultaneously.

Finally, the analysis of the structure shows that the SOS2 PPI binding domain would define a scaffold module involved in the interaction with phosphatases that is structurally conserved from yeast to human.

EXPERIMENTAL PROCEDURES

Protein Expression and Crystallization

Details of the expression and purification of the C-SOS2:SOS3 complex will be published elsewhere. To summarize, the *Arabidopsis thaliana* (*At*) SOS3 (amino acids 1–207) and the *At*SOS2 regulatory domain (amino acids 304–446) were constructed and cloned into the pETDuet plasmid (Novagen). This plasmid was transformed into the *E. coli* BL21-CodonPlus (DE3) (Stratagene) for protein coexpression. The overexpressed proteins were purified in two steps. First, after the cells were disrupted, the clarified supernatant was loaded onto a Resource-S cationic exchange column (Amersham Biosciences Limited, UK) and eluted in a NaCl linear gradient from 50 mM to 0.5 M. Second, the fractions enriched in the C-SOS2:SOS3 complex were then loaded in a gel filtration HiLoad 16/60 Superdex 200 column (GE Healthcare) equilibrated with buffer 20 mM Tris-HCl (pH 8.0), 125 mM NaCl, 5 mM dithiothreitol, 5 mM $CaCl_2$, and 0.05% NaN_3. The protein complex was concentrated to a final concentration of 10 mg/ml.

Crystallization experiments were carried out at room temperature. Crystals corresponding to the C-SOS2:SOS3 complex were grown using vapor diffusion techniques from drops containing C-SOS2:SOS3 (10.0 mg/ml), reservoir solution (20% w/v PEG4000, 0.1 M Tris-HCl [pH 7.5], 0.2 M lithium sulfate, 3% v/v ethylen glycol), and 1 M guanidine HCl in a ratio of 1:1:0.5.

In Vitro Binding Assay

SOS2, SOS3, and ABI2 were cloned in pMALc2x (New England Biolab), pGEX2TK (Amersham), and pET14b (Novagen), respectively. Recombinant proteins were expressed in *E. coli* Rosetta cells (Novagen) and purified using amylose resin (NEB), glutathione-agarose beads (Sigma), or Ni-NTA agarose beads (Qiagen). Eluted GST-SOS3, His-ABI2, and GST were dialyzed with 10 mM Tris-HCl (pH 8.0), and 150 mM NaCl for 12 hr. MBP-SOS2 (4 μg) bound to amylose beads was incubated without or with different amounts of His-ABI2 or BSA (0.2, 1.2, 6, and 30 μg) in binding buffer (10 mM Tris-HCl [pH 8.0], 150 mM NaCl, 1 mM $CaCl_2$, 0.1% Nonidet-P40) at 4°C for 90 min. Then the beads were washed twice with 210 volumes of binding buffer and incubated with GST-SOS3 (4 μg) at 4°C for 60 min. Again, the beads were washed three times with 20 volumes of binding buffer. The bound proteins were eluted with Laemmli sample buffer. The samples were subjected to SDS-polyacrylamide gel electrophoresis and transferred to nitrocellulose membranes (Amersham). After blocking with 5% skim milk, membranes were incubated with anti-GST antibody (Amersham) in phosphate-buffered saline containing 0.1% Tween-20 and subsequently with horseradish peroxidase-conjugated anti-goat IgG antibody (Sigma). Immunoreactive bands were detected by the ECL western blotting detection system (Amersham). For the quantitative analysis, the intensity of the bands was measured with ImageJ.

Data Collection, Structure Determination, and Refinement

Crystals were transferred to a solution containing 25% glycerol and mounted in a fiber loop and frozen at 100 K in a nitrogen stream. X-ray diffraction data were collected in a CCD detector using the ESRF Grenoble synchrotron radiation source at ID29 beamline. Diffraction data were processed using MOSFLM (Leslie, 1987). Data collection statistics are summarized in Table 1.

The X-ray structure of C-SOS2:SOS3 complex was solved by molecular replacement at 2.0 Å using the coordinates of the X-ray structure of the unbound SOS3 (AMoRe) (Navaza, 1994). The electron density map calculated using these phases was good enough to manually build and refine the residues of the SOS3 moiety of the complex. Starting with this preliminary model, most of the residues from C-SOS2 could be traced automatically using ARP/wARP (Perrakis et al., 1997). A complete model of the C-SOS2:SOS3 complex was refined using the simulated annealing routine of CNS (Brunger and Adams, 1998). Several cycles of restrained refinement with REFMAC5 (Murshudov et al., 1997) and iterative model building with O (Jones et al., 1991) were carried out. Calculations were performed using CCP4 programs (CCP4, 1994). The stereochemistry of the model was verified with PROCHECK (Laskowski et al., 1993). Ribbon figures were produced using PyMOL (DeLano, 2002). The accessible surface area calculations were performed with the program "naccess" from LIGPLOT package (Wallace et al., 1995). The refinement statistics are summarized in Table 1.

Sedimentation Equilibrium Experiments

Sedimentation equilibrium experiments were performed in a Beckman Optima XL-A ultracentrifuge using a Ti50 rotor and six channel centerpieces of Epon charcoal (optical pathlength 12 mm). Samples of C-SOS2:SOS3 were equilibrated against 20 mM Tris-HCl (pH 7.5) and 50 mM NaCl buffer plus 5 mM $CaCl_2$ or 1 mM EDTA and were centrifuged at 17,000, 20,000 and 29,000 rpm at 20°C. Radial scans at 280 nm were taken at 12, 14, and 16 hr. The three scans were identical (equilibrium conditions were reached). The weight-average molecular mass (M_w) of C-SOS2:SOS3 was determined by using the program EQASSOC with the partial specific volume of C-SOS2:SOS3 set to 0.730 at 20°C as calculated from its amino acid composition. Calculations were performed with data at 17,000 rpm.

Supplemental Data

Supplemental Data include three figures and one movie and can be found with this article online at http://www.molecule.org/cgi/content/full/26/3/427/DC1/.

ACKNOWLEDGMENTS

We thank Dr. J.L. Saiz-Velasco for the analytical ultracentrifugation data analysis and Dr. Philip R. Evans for critical reading of the manuscript. M.J.S.-B. was supported by a Formacion de Personal Investigador studentship from Ministerio de Educación, Cultura y Deporte, and a Postgraduate I3P Fellowship from the Consejo Superior de Investigaciones Cientificas. A.A. thanks the European Synchrotron Radiation Facility (ESRF) for access to the synchrotron radiation source. This work was funded by the BFU2005-06388-C04-02/BMC grant of the Spanish "Plan Nacional" (MEC) and "Factoría de Cristalización" Consolider Ingenio 2010 to A.A. and by U.S. National Institutes of Health grant R01GM59138 to J.-K.Z.

Received: November 17, 2006
Revised: March 6, 2007
Accepted: April 13, 2007
Published: May 10, 2007

REFERENCES

Batistic, O., and Kudla, J. (2004). Integration and channeling of calcium signaling through the CBL calcium sensor/CIPK protein kinase network. Planta *219*, 915–924.

Ben-Ammar, Y., Takeda, S., Hisamitsu, T., Mori, H., and Wakabayashi, S. (2006). Crystal structure of CHP2 complexed with NHE1-cytosolic region and an implication for pH regulation. EMBO J. *25*, 2315–2325.

Brunger, A.T., and Adams, P.D. (1998). Crystallography and NMR system. Acta Crystallogr. D Biol. Crystallogr. *54*, 905–921.

CCP4 (Collaborative Computational Project, Number 4). (1994). The CCP4 suite: programs for protein crystallography. Acta Crystallogr. D Biol. Crystallogr. *50*, 760–763.

DeLano, W.I. (2002). The PyMOL User's Manual (San Carlos, CA: DeLano Scientific).

Gong, D., Guo, Y., Schumaker, K.S., and Zhu, J.K. (2004). The SOS3 family of calcium sensors and SOS2 family of protein kinases in Arabidopsis. Plant Physiol. *134*, 919–926.

Guo, Y., Halfter, U., Ishitani, M., and Zhu, J.K. (2001). Molecular characterization of functional domains in the protein kinase SOS2 that is required for salt tolerance. Plant Cell *13*, 1383–1399.

Guo, Y., Qiu, Q.S., Quintero, F.J., Pardo, J.M., Ohta, M., Zhang, C., Schumaker, K.S., and Zhu, J.K. (2004). Transgenic evaluation of activated mutant alleles of SOS2 reveals a critical requirement for its kinase activity and C-terminal regulatory domain for salt tolerance in *Arabidopsis thaliana*. Plant Cell *16*, 435–449.

Halfter, U., Ishitani, M., and Zhu, J.K. (2000). The Arabidopsis SOS2 protein kinase physically interacts with and is activated by the calcium-binding protein SOS3. Proc. Natl. Acad. Sci. USA *97*, 3735–3740.

Harmon, A.C., Gribskov, M., and Harper, J.F. (2000). CDPKs—a kinase for every Ca2+ signal? Trends Plant Sci. *5*, 154–159.

Ishitani, M., Liu, J., Halfter, U., Kim, C.S., Shi, W., and Zhu, J.K. (2000). SOS3 function in plant salt tolerance requires N-myristoylation and calcium binding. Plant Cell *12*, 1667–1678.

Jin, L., and Harrison, S.C. (2002). Crystal structure of human calcineurin complexed with cyclosporin A and human cyclophilin. Proc. Natl. Acad. Sci. USA *99*, 13522–13526.

Jones, T.A., Zon, J.Y., Cowan, S.W., and Kjeldgaard, M. (1991). Improved methods for model building in electron density maps and the location of errors in these models. Acta Crystallogr. A *47*, 110–119.

Kissinger, C.R., Parge, H.E., Knighton, D.R., Lewis, C.T., Pelletier, L.A., Tempczyk, A., Kalish, V.J., Tucker, K.D., Showalter, R.E., Moomaw, E.W., et al. (1995). Crystal-structures of human calcineurin and the human FKBP12-FK506-calcineurin complex. Nature *378*, 641–644.

Landau, M., Mayrose, I., Rosenberg, Y., Glaser, F., Martz, E., Pupko, T., and Ben-Tal, N. (2005). ConSurf: the projection of evolutionary conservation scores of residues on protein structures. Nucleic Acids Res *33*, W299–W302.

Laskowski, R.A., MacArthur, M.W., Moss, D.S., and Thornton, J.M. (1993). PROCHECK, a program to check the stereochemical quality of protein structures. J. Appl. Crystallogr. *26*, 283–291.

Leslie, A.G.W. (1987). MOSFLM. In Proceedings of the CCP4 Study Weekend., J.R. Machin and M.Z. Papiz, eds. (Warrington, UK: SERC Daresbury Laboratory), pp. 39–50.

Lewit-Bentley, A., and Rety, S. (2000). EF-hand calcium-binding proteins. Curr. Opin. Struct. Biol. *10*, 637–643.

Li, L., Kim, B.G., Cheong, Y.H., Pandey, G.K., and Luan, S.A. (2006). Ca(2)+ signaling pathway regulates a K(+) channel for low-K response in Arabidopsis. Proc. Natl. Acad. Sci. USA *103*, 12625–12630.

Liu, J., and Zhu, J.K. (1998). A calcium sensor homolog required for plant salt tolerance. Science *280*, 1943–1945.

Liu, J., Ishitani, M., Halfter, U., Kim, C.S., and Zhu, J.K. (2000). The *Arabidopsis thaliana SOS2* gene encodes a protein kinase that is required for salt tolerance. Proc. Natl. Acad. Sci. USA *97*, 3730–3734.

Luan, S., Kudla, J., Rodriguez-Concepcion, M., Yalovsky, S., and Gruissem, W. (2002). Calmodulins and calcineurin B-like proteins, calcium sensors for specific signal response coupling in plants. Plant Cell *14*, S389–S400.

Moscat, J., Diaz-Meco, M.T., Albert, A., and Campuzano, S. (2006). Cell signaling and function organized by PB1 domain interactions. Mol. Cell *23*, 631–640.

Murshudov, G.N., Vagin, A.A., and Dodson, E.J. (1997). Refinement of macromolecular structures by the maximum-likelihood method. Acta Crystallogr. D Biol. Crystallogr. *53*, 240–255.

Nagae, M., Nozawa, A., Koizumi, N., Sano, H., Hashimoto, H., Sato, M., and Shimizu, T. (2003). The crystal structure of the novel calcium-binding protein AtCBL2 from *Arabidopsis thaliana*. J. Biol. Chem. *278*, 42240–42246.

Navaza, J. (1994). AMoRe, an automated package for molecular replacement. Acta Crystallogr. A *50*, 157–163.

Ohta, M., Guo, Y., Halfter, U., and Zhu, J.K. (2003). A novel domain in the protein kinase SOS2 mediates interaction with the protein phosphatase 2C ABI2. Proc. Natl. Acad. Sci. USA *100*, 11771–11776.

Otterbein, L.R., Kordowska, J., Witte-Hoffmann, C., Wang, C.L., and Dominguez, R. (2002). Crystal structures of S100A6 in the Ca(2+)-free and Ca(2+)-bound states, the calcium sensor mechanism of S100 proteins revealed at atomic resolution. Structure *10*, 557–567.

Perrakis, A., Sixma, T.K., Wilson, K.S., and Lamzin, V.S. (1997). wARP: improvement and extension of crystallographic phases by weighted averaging of multiple-refined dummy atomic models. Acta Crystallogr. D Biol. Crystallogr. *53*, 448–455.

Qiu, Q., Guo, Y., Dietrich, M.A., Schumaker, K.S., and Zhu, J.K. (2002). Regulation of SOS1, a plasma membrane Na^+/H^+ exchanger in *Arabidopsis thaliana*, by SOS2 and SOS3. Proc. Natl. Acad. Sci. USA *99*, 8436–8441.

Quintero, F.J., Ohta, M., Shi, H., Zhu, J.K., and Pardo, J.M. (2002). Reconstitution of the SOS signaling pathway for Na^+ homeostasis in plants. Proc. Natl. Acad. Sci. USA *99*, 9061–9066.

Sanchez-Barrena, M.J., Martinez-Ripoll, M., Zhu, J.K., and Albert, A. (2005). The structure of the *Arabidopsis thaliana* SOS3: molecular mechanism of sensing calcium for salt stress response. J. Mol. Biol. *345*, 1253–1264.

Scrase-Field, S.A., and Knight, M.R. (2003). Calcium, just a chemical switch? Curr. Opin. Plant Biol. *6*, 500–506.

Tassan, J.P., and Le Goff, X. (2004). An overview of the KIN1/PAR-1/MARK kinase family. Biol. Cell. *96*, 193–199.

Tochio, N., Koshiba, S., Kobayashi, N., Inoue, M., Yabuki, T., Aoki, M., Seki, E., Matsuda, T., Tomo, Y., Motoda, Y., et al. (2006). Solution structure of the kinase-associated domain 1 of mouse microtubule-associated protein/microtubule affinity-regulating kinase 3. Protein Sci. *15*, 2534–2543.

Wallace, A.C., Laskowski, R.A., and Thornton, J.M. (1995). LIGPLOT, a program to generate schematic diagrams of protein-ligand interactions. Protein Eng. *8*, 127–134.

Xu, J., Li, H.D., Chen, L.Q., Wang, Y., Liu, L.L., He, L., and Wu, W.H. (2006). A protein kinase, interacting with two calcineurin B-like proteins, regulates K+ transporter AKT1 in Arabidopsis. Cell *125*, 1347–1360.

Zhu, J.K. (2000). Genetic analysis of plant salt tolerance using *Arabidopsis thaliana*. Plant Physiol. *124*, 941–948.

Zhu, J.K. (2003). Regulation of ion homeostasis under salt stress. Curr. Opin. Plant Biol. *6*, 441–445.

Accession Numbers

The coordinates and structure factor amplitudes of the C-SOS2:SOS3 complex have been deposited in the Protein Data Bank under ID code 2EHB.